Original Study

Diagnostic Utility of RNA-Seq for Evaluation of PD-L1 Expression in Clear Cell Renal Cell Carcinoma

Maria Sorokina,[1] Danil Stupichev,[1] Yang Lyu,[2] Akshaya Ramachandran,[2] Natalia Miheecheva,[1] Jessica H. Brown,[1] Krystle Nomie,[1] Ekaterina Postovalova,[1] Alexander Bagaev,[1] Maria Tsiper,[1] James J. Hsieh[2]

Abstract

This study was designed to determine the ability of RNA-Seq to detect PD-L1 expression in comparison with IHC in clear cell renal cell carcinoma (ccRCC). Analysis of 127 ccRCC clinical samples demonstrated that RNA-Seq can detect PD-L1 expression as accurately as IHC. These results suggest that PD-L1 detection by RNA-Seq can be further developed for clinical utility in ccRCC.

Background: Although there are immune checkpoint inhibitors (ICIs) available for the treatment of renal cell carcinoma (RCC), the utility of PD-L1 detection by immunohistochemistry (IHC) as a predictive biomarker in clear cell RCC (ccRCC) remains controversial. Nevertheless, alternative methods for PD-L1 detection, such as RNA sequencing (RNA-Seq), may be clinically useful in ccRCC; therefore, we sought to determine the ability of RNA-Seq to accurately and sensitively detect PD-L1 expression across different ccRCC clinical samples in comparison with IHC. **Patients and Methods:** Patients with ccRCC (n=127) who received treatment from Washington University in St. Louis between 2018 and 2020 were identified. Tumors from these patients were analyzed using RNA-Seq and IHC. **Results:** PD-L1 detection by RNA-Seq strongly correlated with IHC ($P < .001$), which was further validated using two independent datasets. Furthermore, RNA-Seq analysis identified an immune-enriched (higher PD-L1 positivity) and an immune-desert (lower PD-L1 positivity) microenvironment of ccRCC, which also correlated with IHC ($P < .00001$). **Conclusion:** The results demonstrate the ability of RNA-Seq to detect PD-L1 in various ccRCC clinical samples compared to IHC. Ultimately, these findings suggest that PD-L1 detection by RNA-Seq can be further developed to determine the clinical utility of this methodology in ccRCC.

Clinical Genitourinary Cancer, Vol. 000, No.xxx, 1–8 © 2021 Published by Elsevier Inc.
Keywords: Immunohistochemistry, Tumor microenvironment, Programmed death ligand 1, RNA-Sequencing, Clear Cell Renal Cell Carcinoma

Introduction

Renal cell carcinoma (RCC), one of the top ten most commonly diagnosed cancers worldwide,[1] encompasses a large heterogeneous group of cancers derived from renal tubular epithelial cells and accounts for more than 90% of cancers detected in the kidney.[2–4] Clear cell renal cell carcinoma (ccRCC) is the predominant histology of RCC, representing 75% of all cases.[5] A decrease in the 5-year survival rate for patients with ccRCC is strongly associated with the advancement of disease, highlighting the critical need for early detection and optimal treatment selection.[6] Harnessing the immune system through the inhibition of immune checkpoint molecules has demonstrably altered the field of cancer therapy, including that of ccRCC. The blockade of immune checkpoints with immune checkpoint inhibitors (ICIs), such as programmed death ligand 1 (PD-L1) neutralizing antibody, has been shown to be a highly effective treatment for ccRCC.[7] PD-L1, a transmembrane cell surface protein expressed on both tumor and immune cells of the tumor microenvironment (TME), inhibits the T-cell immune response, allowing cancer cells to evade the immune system. Although immunohistochemical (IHC) PD-L1 scoring of immune and/or tumor cells (IC/TC) is used for immune checkpoint therapy stratification, the utility of PD-L1 detection by IHC based on various FDA-approved anti-PD-L1 antibodies in predicting treatment outcomes has been

Conflict of Interest: Background: JJH has received consulting fees from Eisai and BostonGene; clinical trial funding from BMS, Merck USA, AstraZeneca, Exelixis, and SillaJen; and research funding from Merck USA, BostonGene, and TScan.

[1] BostonGene Corporation, Waltham, MA
[2] Department of Medicine, Division of Oncology, Washington University School of Medicine, St. Louis, MO

Submitted: Apr 1, 2021; Revised: Jun 17, 2021; Accepted: Jul 2, 2021; Epub: xxx

Address for correspondence: James Hsieh, MD, PhD, Division of Oncology, Department of Internal Medicine, Washington University School of Medicine, 660 S. Euclid Ave, Box 8069, St. Louis, MO 63110, USA
E-mail contact: jhsieh@wustl.edu

1558-7673/$ - see front matter © 2021 Published by Elsevier Inc.
https://doi.org/10.1016/j.clgc.2021.07.010

Please cite this article as: Maria Sorokina et al, Diagnostic Utility of RNA-Seq for Evaluation of PD-L1 Expression in Clear Cell Renal Cell Carcinoma, Clinical Genitourinary Cancer, https://doi.org/10.1016/j.clgc.2021.07.010

controversial in ccRCC, as it has correlated with poorer survival but not with patient response to immune checkpoint blockade.[8,9]

This inability of PD-L1 to be utilized as a biomarker in ccRCC may be due to shortcomings of the IHC assays, opening the door for other methodologies to be assessed as potential alternatives for PD-L1 detection. A recent meta-analysis comparing the diagnostic accuracy of 22 studies performing PD-L1 IHC assays suggests that since no prospective clinical trials have been conducted to compare IHC assays, the assays cannot be deemed "interchangeable". This meta-analysis also highlighted the absence of tools to measure the analytical sensitivity and specificity of IHC assays, which can lead to problems in the daily monitoring of assay performance as well as its calibration.[10] The current lack of data comparing different IHC assays of PD-L1 expression in ccRCC highlights the need for the utilization of alternative detection methods.

Recently, due to the advancement of next-generation sequencing (NGS) techniques, RNA-Seq technology is actively being evaluated as a more robust and highly automated method for PD-L1 expression. However, for the wide implementation of RNA-Seq-derived values of PD-L1 expression in clinical practice, it is necessary to compare the values obtained *via* the different RNA-Seq and IHC technologies. Therefore, in this study, the correlation between PD-L1 mRNA expression computed from RNA-Seq and classical PD-L1 protein detection *via* IHC in ccRCC formalin-fixed paraffin-embedded (FFPE) tumor samples was investigated. Additionally, PD-L1 status in relation to microenvironment subtyping was examined using ccRCC samples to ascertain a potential link between PD-L1 expression and different TME classifications.

Materials and Methods

Patient and Specimen Collection

This study was approved by the Institutional Review Board at Washington University Medical School in St. Louis. Eligibility criteria for the collection of samples included histologically confirmed ccRCC. Informed consents from patients were obtained prior to sample collection. The WUSMRCC cohort included 127 patients with corresponding PD-L1 IHC values for tumor and immune cells. The bio-specimens and clinical data used in this study were provided by Washington University Medical School in St. Louis. Baseline demographic and clinical characteristics of the ccRRC cohort were collected prior to sample collection. We validated our results using JAVELIN (N=726; NCT02684006)[11] and Mariathasan (NCT02108652)[12] datasets. We excluded the basal-squamous-like (BASQ) subtype from Mariathasan cohort as the expression of PD-L1 in this particular subtype is significantly higher than in the rest of Muscle-Invasive Urinary Bladder Urothelial Carcinomas[13] (N=281 after filtering).

Immunohistochemistry (IHC)

Fresh ccRCC tissue specimens were fixed after dissection with 10% formalin for 48 hours at room temperature. Tissue specimens were dehydrated by immersing specimens in a series of ethanol solutions of increasing concentration: 70% (1x), 80% (1x), 95% (1x), and 100% (2x) for 1 hour each. The specimens were then immersed in fresh-xylene (or xylene substitute) three times for 1.5 hours each, followed by immersion in paraffin wax (58 ^{0}C-60 ^{0}C) twice for 2 hours each. Next, the tissue specimens were embedded into paraffin blocks. Tissue sections (5 µm thick) were cut from FFPE tissue blocks using a microtome and then mounted onto Superfrost Ultra Plus adhesion slides for morphological examination. Slide tissue sections were baked at 60 ^{0}C in an oven for 1 hour. The tissue sections were deparaffinized with 2 washes of fresh-xylene. Then, the tissue sections were rehydrated with washes of ethanol 100% (2x), 95% (2x), 70% (2x), 50% (2x), 1X PBS (1x), and 0.3% Triton X100 in 1X PBS (1x) and subjected to a two-step antigen retrieval process. The sections were stained with antibodies (Dako 22C3, Ventana SP263 and Ventana SP142) at a previously optimized concentration.

Transcriptome Sequencing and Data Analysis

Total RNA was extracted from FFPE samples. RNA-Seq FASTQ data and values of PD-L1 from IHC staining were provided by Washington University at St. Louis. RNA-Seq and PD-L1 IHC testing was performed by Tempus using the xT test (PD-L1 IHC 22C3 parmDx was used [clone 22C3]). PD-L1 IHC test results were obtained as a percentage of PD-L1 positive cells per a population of tumor cells and tumor-associated immune cells (mono-nucleated inflammatory cells in tumor proximity). PD-L1 in humans is encoded by the *CD274* gene. Sequenced reads were aligned to the human reference genome hg38 using Kallisto version 0.42.4 with GENCODE v23 transcripts.[14] Only protein coding transcripts were left for normalization. Gene expressions were measured as transcripts per million (TPM).

Gene Expression Signatures Describing the TME And Tumor Properties

Gene signatures that reflect the main processes in the TME were constructed, and single sample gene set enrichment analysis (ssGSEA) scores for these signatures were calculated; the scores within each cohort were medium-scaled. Immune-enriched and immune-desert clusters were identified by graph clustering of the scores. To gain more statistical power, clusters were identified on a meta-cohort made of 1,675 samples from various datasets (GSE2109, GSE53757, GSE46699, GSE73731, GSE40435, GSE17818, GSE17816, TCGA KIRC, ICGC RECA-EU, CPTAC-3 Kidney, EGAS00001000509, and phs001493).

Purified Cell Type Compendium

We collected 7,071 RNA-Seq gene expression datasets from purified cell populations, including normal and melanoma cells from the following public data sources to create a cell compendium: GEO,[15] SRA,[16] ENA, Array Express, Protein Atlas,[17] BluePrint, ImmPort [immport.org]). We included datasets using the following criteria: isolated from human tissue, poly-A or total RNA-Seq performed with read length higher than 31 bp, having at least 4M of coding read counts, passed quality control by FASTQC version 0.11.9 and no contamination detected (< 2%). The compendium included sorted T cells, CD4+ T cells, T regulatory cells (T-regs), T helper cells, T follicular helper cells (TFH), CD8+ T cells, NK cells, benign B cells, granulocytes of different types, neutrophils, macrophages, monocytes, myeloid cells, dendritic cells, plasmacytoid dendritic cells, vascular and lymphatic endothelial cells (VEC,

Please cite this article as: Maria Sorokina et al, Diagnostic Utility of RNA-Seq for Evaluation of PD-L1 Expression in Clear Cell Renal Cell Carcinoma, Clinical Genitourinary Cancer, https://doi.org/10.1016/j.clgc.2021.07.010

Table 1 Baseline Demographic and Clinical Characteristics of the WUSMRCC Cohort

Characteristic (total) N=127	Quantifiable tumor PD-L1 expression			Quantifiable immune cell PD-L1 expression		
	<1%	≥1%	*P*-value	<1%	≥1%	*P*-value
Median age at 1st RCC diagnosis (range) — yr	60 (19–87)	59 (31–83)	0.59	62 (19–84)	57 (31-87)	0.41
Sex — no. (%)						
Male (N=84)	60 (71%)	24 (29%)	0.28	43 (52%)	41 (48%)	0.09
Female (N=43)	35 (81%)	8 (19%)		29 (67%)	14 (33%)	
IMDC prognostic risk — no. (%)*						
Favorable (N=67)	55 (82%)	12 (18%)	0.07	37 (55%)	30 (45%)	0.88
Intermediate (N=47)	33 (70%)	14 (30%)		28 (60%)	19 (40%)	
Poor (N=13)	7 (54%)	6 (46%)		7 (54%)	6 (46%)	
Previous radiotherapy — no. (%)	0	0		0	0	
Previous nephrectomy (N=113) — no. (%)	85 (75%)	28 (25%)	0.75	63 (56%)	50 (44%)	0.58
Most common sites of metastasis — no. (%)						
Lung (N=53)	33 (62%)	20 (38%)	0.03	27 (51%)	26 (49%)	0.28
Lymph node (N=21)	13 (62%)	8 (38%)	0.28	10 (48%)	11 (52%)	0.46
Bone (N=33)	23 (70%)	10 (30%)	0.81	21 (64%)	12 (36%)	0.28
Brain (N=14)	10 (71%)	4 (29%)	1.0	12 (86%)	2 (14%)	0.02

IMDC: International Metastatic Renal Cell Carcinoma Database Consortium; PD-L1: programmed death ligand 1.
* Patients with favorable risk had an IMDC score of 0, those with intermediate risk had a score of 1 or 2, and those with poor risk had a score of 3 to 6. IMDC risk scores are defined by the number of the following risk factors present: a Karnofsky performance-status score of 70 (on a scale from 0 to 100, with lower scores indicating greater disability), a time from initial diagnosis to randomization of less than 1 year, a hemoglobin level below the lower limit of the normal range, a corrected serum calcium concentration of more than 10 mg per deciliter (2.5 mmol per liter), an absolute neutrophil count above the upper limit of the normal range, and a platelet count above the upper limit of the normal range.

LEC), and fibroblasts. An "activated macrophages" group of cells were selected from samples of macrophages activated with bacteria or LPS, according to annotation. Sorted melanoma tumor cells and cell lines were included for comparison.

Louvain Clustering

The Pearson correlation [-1, 1] was calculated between the samples in the space of the 29 process intensities (normalized ssGSEA enrichment scores). Next, the distance matrix was converted into a graph where each sample formed a node and two nodes formed an edge with the weight equal to their Pearson correlation. All edges with weight < 0.45 were removed. The Louvain community detection algorithm[18] was utilized to partition into clusters with default parameters. To mathematically determine the optimal weight threshold for observed clusters, minimum Davies–Bouldin, maximum Calinski-Harabasz, and Silhouette scores were employed. Separations with low populated clusters (< 5% of samples) were not considered.

Results

To compare the sensitivity and clinical utility of RNA-Seq and IHC in PD-L1 detection, a total of 127 ccRCC tumors collected from patients treated at Washington University in St. Louis were analyzed in this study (WUSMRCC cohort). Metastatic and inoperable advanced ccRCC patients were treated with ipilimumab plus nivolumab (IPI + NIVO), anti-PD-1 antibody + tyrosine kinase inhibitor (TKI), or TKI alone. Table 1 lists the demographic and clinical characteristics of the patients from which the ccRCC tumors were obtained. At the time of sample collection, the majority of patients (113 of 127, 89%) had undergone a nephrectomy. A large portion of patients had metastatic disease, with the most frequent sites of metastasis occurring in the lung (42%), lymph nodes (17%), bones (26%), and brain (11%). All specimens were re-evaluated by an experienced uropathologist according to the latest TNM and WHO classification. The specimens were primary or metastatic tumors, including core needle biopsies.

The resected or biopsy samples at Washington University were analyzed *via* RNA-Seq and IHC using Dako 22C3 antibody for PD-L1. For the IHC-based assay, PD-L1 expression was evaluated by counting PD-L1-positive cells (percent of PD-L1-expressing cells within the tumor and within mononucleated inflammatory cells in tumor proximity assays). PD-L1 expression computed based on RNA-Seq deconvolution of PD-L1 transcripts strongly correlated with the PD-L1 values obtained *via* IHC ($P < .001$; Figure 1A). We then used two independent datasets to validate these results. The first dataset consisted of tumor samples from the phase 3 JAVELIN Renal 101 trial (N=726; NCT02684006), which demonstrated prolonged progression-free survival (PFS) with first-line avelumab + axitinib versus sunitinib in advanced renal cell carcinoma (aRCC). PD-L1 measured by IHC using Ventana SP263 antibody in the JAVELIN dataset correlated with our PD-L1 data measured by RNA-Seq ($P < .001$; Figure 1B). The second dataset was composed of a large cohort of patients (Mariathasan cohort; NCT02108652) with metastatic urothelial cancer who were treated with an anti-PD-L1 agent, atezolizumab. Again, PD-L1 measured by IHC using the Ventana SP142 antibody in the Mariathasan cohort also correlated with PD-L1 measured by RNA-Seq ($P < .001$; Figure 1C). Due to the variable methodology for IHC PD-L1 detection, different cut-off values were used (≥1% for Mariathasan and WUSMRCC cohorts and ≥ 2% for the JAVELIN dataset).

To understand the relationship between PD-L1 expression levels of individual tumors and TMEs, knowledge-based gene expres-

Please cite this article as: Maria Sorokina et al, Diagnostic Utility of RNA-Seq for Evaluation of PD-L1 Expression in Clear Cell Renal Cell Carcinoma, Clinical Genitourinary Cancer, https://doi.org/10.1016/j.clgc.2021.07.010

Please cite this article as: Maria Sorokina et al, Diagnostic Utility of RNA-Seq for Evaluation of PD-L1 Expression in Clear Cell Renal Cell Carcinoma, Clinical Genitourinary Cancer, https://doi.org/10.1016/j.clgc.2021.07.010

Figure 1 PD-L1 RNA expression from RNA-Seq correlates with PD-L1 protein expression from IHC.
A. Box plots showing PD-L1 expression levels calculated by RNA-Seq per ccRCC sample categorized as having PD-L1-positive malignant tumor cells with ≥1% or <1% or PD-L1-positive immune cells with ≥1% or <1% as determined by IHC. The boxes in the box plot represent the interquartile range (IQR), where the centerline depicts the median. The upper whisker indicates the maximum value or 75th percentile +1.5 IQR, whichever is smaller; the lower whisker indicates the minimum value or 25th percentile -1.5 IQR, whichever is greater. RNA-Seq expression was clipped to the interval 0-4 TPM (transcripts per million). P-values were calculated with the Mann-Whitney U test.
B. Validation on a cohort of patients with advanced renal cell carcinoma (aRCC) (Motzer et al. 2020). RNA-Seq expression was clipped to the interval 0-8 TPM. P-values were calculated with the Mann-Whitney U test.
C. Validation on a cohort of patients with metastatic urothelial cancer (Mariathasan et al. 2018). RNA-Seq expression was clipped to the interval 0-5 TPM. P-values were calculated with the Mann-Whitney U test.

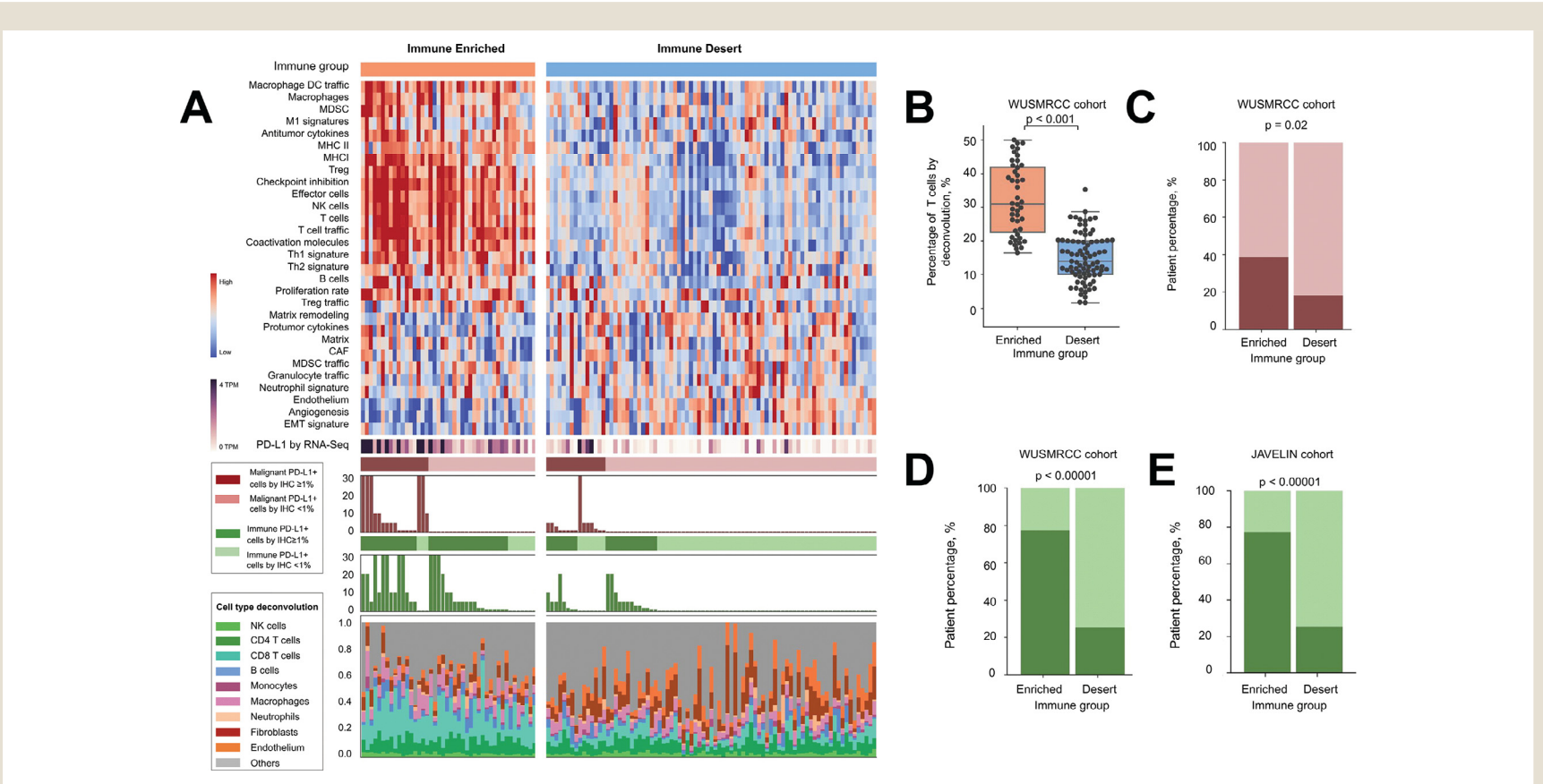

Figure 2 PD-L1 positive immune cells are significantly associated with higher immune cell populations via deconvolution.
A. Top, heatmap of the WUSMRCC cohort classified into two distinct TME subtypes (immune enriched [peach] and immune desert [blue]) based on unsupervised dense clustering of the 29 gene expression signatures. PD-L1 expression measured by RNA-Seq in each sample is highlighted as purple color gradient. Middle, bar graphs showing the percentage of the number of malignant [purple] and immune [green] PD-L1+ cells per ccRCC samples. Bottom, bar plot showing the percentage of each cell type per ccRCC sample.
B. Box plots representing percentage of T cells by deconvolution in Enriched and Desert immune groups. P-values were calculated with the Mann-Whitney U test.
C. Bar graphs showing the percentage of PD-L1-positive malignant cells (≥1%) detected by IHC per TME subtype in WUSMRCC cohort. *P*-values were obtained from Pearson's chi-square test.
D. Bar graphs showing the percentage of PD-L1-positive immune cells (≥1%) detected by IHC per TME subtype in WUSMRCC cohort. *P*-values were obtained from Pearson's chi-square test.
E. Bar graphs showing the percentage of PD-L1-positive immune cells (≥2%) detected by IHC per TME subtype in JAVELIN cohort. *P*-values were obtained from Pearson's chi-square test.

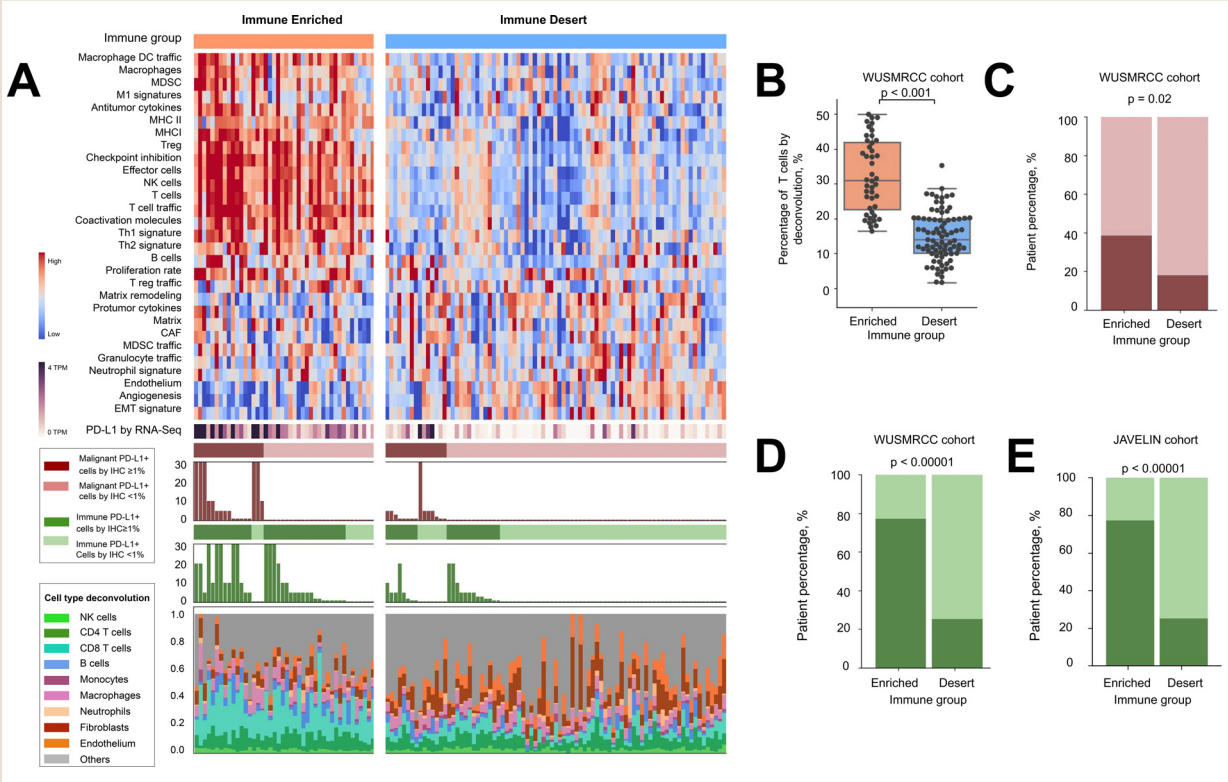

sion signatures were used to comprehensively characterize the ccRCC TMEs from RNA-Seq (Figure 2A). This classification system revealed that the ccRCC samples in the WUSMRCC cohort clustered into two distinct microenvironments: an immune-enriched microenvironment with high lymphocyte infiltration and an immune-desert microenvironment predominantly composed of malignant cells ($P < .001$; Figure 2B). The correlations between PD-L1 detection by IHC and the immune microenvironment classifications were also evaluated. Notably, the ccRCC samples in the immune-enriched clusters had a higher percentage of tumors with detectable PD-L1 protein (≥1% for tumor cells IHC, $P = .02$; ≥1% for immune cells IHC, $P < .001$; Figure 2C and 2D, respectively). This observation was also confirmed in the JAVELIN Renal 101 cohort ($P < .001$; Figure 2E). These findings indicate that an immune-enriched TME consists of more PD-L1 expression cells compared to an immune-desert TME.

Next, the ability of PD-L1 detection to predict response to ICIs within the ccRCC patients was investigated. Responders (R) were defined as CR+PR (complete response plus partial response) and non-responders (NR) were defined as SD+PD (stable disease plus progressive disease) using Response Evaluation Criteria in Solid Tumors 1.1. (RECIST version 1.1) methodology. When PD-L1 expression was measured by IHC, a higher PD-L1 level in malignant and immune cells was associated with response to ICIs compared to a lower PD-L1 level that was associated with no response to ICIs (20 R and 28 NR; $P = .08$ for malignant and $P = .03$ for immune cells; Figure 3A). Similarly, higher PD-L1 levels measured by RNA-Seq correlated with response to ICIs (17 R and 22 NR; $P = .02$; Figure 3A). Furthermore, among responders, a significantly

Please cite this article as: Maria Sorokina et al, Diagnostic Utility of RNA-Seq for Evaluation of PD-L1 Expression in Clear Cell Renal Cell Carcinoma, Clinical Genitourinary Cancer, https://doi.org/10.1016/j.clgc.2021.07.010

Figure 3 PD-L1 expression from RNA-Seq correlates with treatment response to ICIs better than PD-L1 expression from IHC.
A. Patients with higher PD-L1 expression (quantified both by RNA-Seq and IHC) demonstrate better response to checkpoint inhibitors. Responders (R) were defined as CR and PR (complete response and partial response); non-responders (NR) were defined as SD and PD (stable disease and progressive disease) using RECIST 1.1 methodology. Dot colors correspond to a certain TME subtype (light blue - immune desert, light orange - immune enriched). PD-L1+ cells by IHC were clipped to the interval 0-60%. RNA-Seq expression was clipped to the interval 0-4 TPM. *P*-values were calculated with the Mann-Whitney U test.
B. Bar graphs showing the percentage of responders and non-responders per TME subtype (immune enriched versus immune desert) in the WUSMRCC cohort. A significantly higher proportion of patients with immune-enriched TME was observed among responders. *P*-values were obtained from Pearson's chi-square test.
C. Response rate to ICIs in a cohort of urothelial carcinoma patients (Mariathasan et al. 2018). Patients with higher PD-L1 expression (quantified by both IHC and RNA-Seq) demonstrate better response to checkpoint inhibitors. BASQ subtype tumors were excluded. P-values were obtained from Pearson's chi-square test.
D. Response rate to ICIs in a cohort of urothelial carcinoma patients (Mariathasan et al. 2018). Patients with higher PD-L1 expression (quantified by RNA-Seq) demonstrate better response to checkpoint inhibitors. BASQ subtype tumors were excluded. RNA-Seq expression was clipped to the interval 0-4 TPM. *P*-values were calculated with the Mann-Whitney U test.

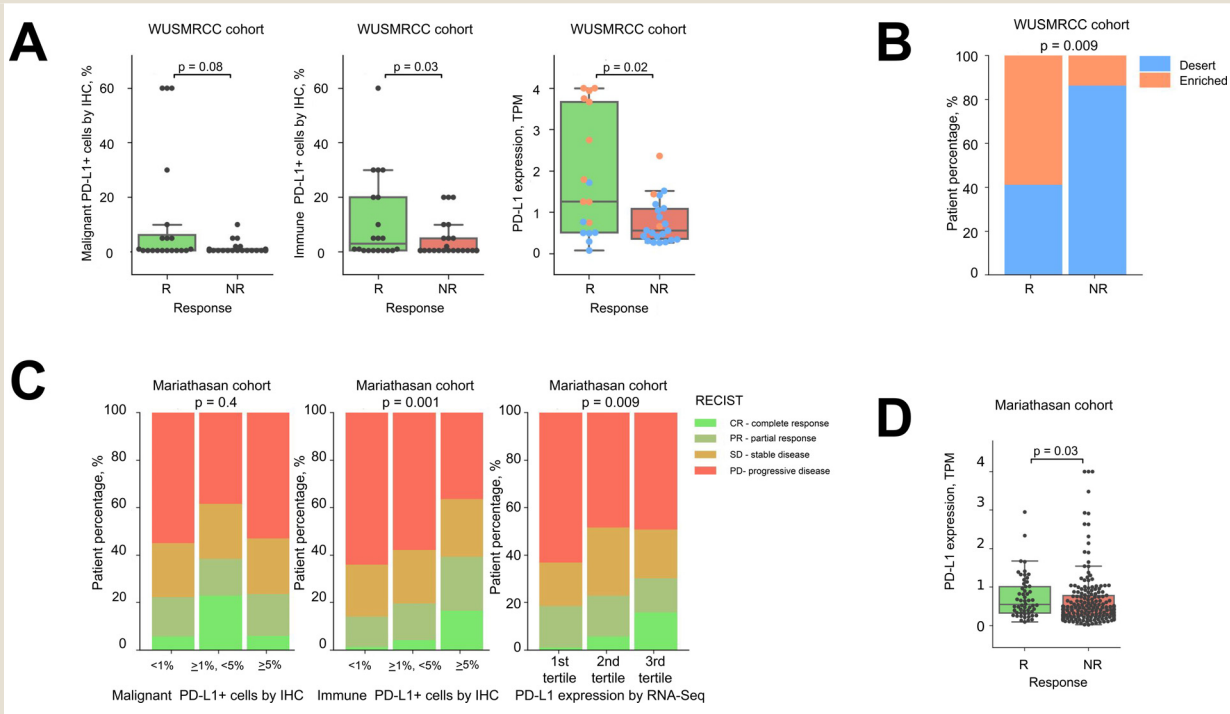

higher proportion of patients with an immune-enriched TME was observed ($P = .009$, Figure 3B).

The Mariathasan et al. cohort was chosen for further analysis. Patients with higher PD-L1 expression quantified by IHC demonstrated a better response to checkpoint inhibitors ($P = .4$ for malignant and $P = .001$ for immune cells; Figure 3C). Similar to our data, PD-L1 expression measured by RNA-Seq is significantly higher in responders compared to non-responders ($P = .03$, Figure 3D). Furthermore, higher PD-L1 levels measured by RNA-Seq were also associated with a better response to ICIs ($P = .009$, Figure 3C). This data suggests that a higher expression of PD-L1 by RNA-Seq could be of value in predicting response to ICIs in the same manner as by IHC in urothelial cancer.

Discussion

The results of this study demonstrate that RNA-Seq deconvolution of PD-L1 transcripts detects PD-L1 expression as accurate as IHC across different ccRCC clinical samples, as well as urothelial cancers. It also harmonizes PD-L1 expression detected by three different commercial anti-PD-L1 antibodies, i.e. Dako 22C3, Ventana SP263, and Ventana SP142. Our experiments further showed that PD-L1-positive cells detected by RNA-Seq deconvolution are significantly associated with an immune-enriched TME encompassing a higher proportion of T cells, which may indicate underlying immune reactions. Finally, we found that PD-L1 expression detected by RNA-Seq associated with treatment response to ICIs better than PD-L1 expression detected from IHC, especially

Please cite this article as: Maria Sorokina et al, Diagnostic Utility of RNA-Seq for Evaluation of PD-L1 Expression in Clear Cell Renal Cell Carcinoma, Clinical Genitourinary Cancer, https://doi.org/10.1016/j.clgc.2021.07.010

compared to tumor cell PD-L1 positivity. Together, the evidence in this study indicates that RNA-Seq detection of PD-L1 can be used as an alternative for PD-L1 detection by IHC in ccRCC clinical samples.

PD-L1 remains a promising biomarker to predict the likelihood of response to ICIs and to estimate prognosis in kidney cancer. Immunotherapeutic agents, particularly ICIs, have shown remarkable efficacy in restoring host immunity against various malignant neoplasms such as ccRCC.[19] Currently, the "gold standard" technique for PD-L1 expression detection is IHC in multiple cancers. Besides the controversial cutoff value of immunohistologic PD-L1 expression, issues compromise its use as a biomarker in ccRCC, including the inconsistent use of several FDA-approved PD-L1 IHC assays in clinical trials and practice. Unsurprisingly, with the availability of multiple *in vitro* diagnostic tests, uncertainty remains regarding the underlying clinical utility and reporting of PD-L1 detection. To address these caveats, the Blueprint study was designed to develop meaningful guidelines for the oncology community that are not based on pre-existing biases of the manufacturers.[20] Despite the Blueprint study involving solely pathologists with considerable expertise, only 50% of the cases demonstrated concordant positive staining among the different IHC assays above the antibody specific cutoffs. Indeed, an additional phase 2 study confirmed variable sensitivity between antibody clones (22C3, 28–8, SP263, SP142) for the IHC assays.[21]

While IHC detection of PD-L1 possesses a number of challenges, RNA-Seq has become largely available and affordable; therefore, the utility of assessing tumor PD-L1 expression *via* RNA-Seq is being explored as an alternative to guide treatment with immunotherapies. A number of retrospective studies have attempted to evaluate the correlation between PD-L1 protein expression and mRNA levels. For example, Eckstein and colleagues investigated PD-L1 expression in a total of 294 non-muscle invasive and muscle-invasive bladder cancer samples through the comparison of RT-qPCR with IHC scoring by three independent pathologists (Dako, 22C3).22 PD-L1 mRNA values and IHC analysis showed a substantial to almost complete agreement ($r = 0.55\text{-}1.00$).[22] An additional study also supported PD-L1 detection *via* RNA-Seq by showing that this method is comparable to IHC and even suggested that RNA-Seq detection of PD-L1 may be superior to IHC in melanoma when performed in a CLIA laboratory environment with a validated protocol. This study further suggested that RNA-Seq has the added advantages of being amenable to standardization and the avoidance of interpretation bias.[23,24] Additional studies have established RNA *in situ* hybridization of PD-L1 as a future gold standard for PD-L1 detection in a large cohort of primary and metastatic bladder carcinomas,[25] further demonstrating the utility of RNA measurement. However, uncertainty surrounding the notion that RNA expression is a reliable alternative to IHC PD-L1 detection exists. For example, a low correlation was observed between RT-PCR and 3 independent PD-L1 IHC assays in the non-small cell lung cancer (NSCLC) CLOVER study.[26]

Here, our comparison of RNA-Seq with PD-L1 detection *via* IHC in the large cohort of ccRCC samples showed a strong correlation between the two methods. Based on the ability to accurately detect PD-L1 expression with RNA-Seq and its inherent advantage of the lower cost of PD-L1 assessment by allowing the testing of several patients in a single sequencing run, RNA-Seq should be considered as a potential viable PD-L1 measurement test in clinical samples of patients with ccRCC. Moreover, correlations were observed among PD-L1 IHC and the microenvironment subtype of the ccRCC samples, suggesting that the comprehensive characterization of the TME may also provide insights into responses to various immunotherapies, including ICIs, which can be further tested and validated with prospective biomarker-based clinical trial designs.

Limitations of this study include a lack of external standards for standardized measurement of PD-L1 expression via RNA-Seq, the lack of publicly-available cohorts that can be used for data normalization, and the required development of an internal proprietary algorithm for the RNA-Seq deconvolution. A common limitation of measuring the expression level from bulk RNA-Seq is the challenge of matching the expression level to the specific cell type. Both malignant and immune cells could express high levels of PD-L1 on the surface. Total RNA-Seq cannot distinguish the expression of PD-L1 among cell types. However, suppression of T-cell function could be mediated by both malignant cells and resident immune cells. Nevertheless, we have shown that the total PD-L1 expression level measured from RNA-Seq exhibits an increased association with response compared to the PD-L1 level measured by IHC in the WUSMRCC cohort. Future methods could possibly delineate the source of the PD-L1 gene expression.

An additional limitation is the lack of a PD-L1 cut-off obtained via RNA-seq for the clinical setting. According to our results, we can speculate that 1 TPM (transcripts per million) is a cut-off of PD-L1 positivity when all values of PD-L1 are concordant with the values obtained *via* IHC with a 1% cut-off (with the exception of outliers) in our WUSMRCC cohort. Moreover, the cut-off may depend on the type of sample used, extraction kit, sequencing platform, and other technical issues of RNA-Seq. PD-L1 measured by RNA-Seq should be used within the laboratory developed test (LDT), or when a comparison cohort is present and obtained in the same way as the sample of interest. Further research is needed to determine the exact PD-L1 threshold for easy comparison with IHC data in routine clinical practice. Another limitation is the retrospective nature of our study. Therefore, future prospective studies will be critical to further validate PD-L1 measurements by RNA-Seq in clinical samples.

Conclusion

Our study describes the ability of RNA-Seq to detect PD-L1 in various ccRCC clinical samples compared to IHC. RNA-Seq analysis identified an immune-enriched (high PD-L1 positivity) and an immune-desert (low PD-L1 positivity) microenvironment of ccRCC, which also correlated with IHC. Our findings suggest that PD-L1 detection by RNA-Seq can be further developed to determine the clinical utility of this methodology in ccRCC. Our data should be further confirmed and future prospective studies will be critical to further validate PD-L1 measurements by RNA-Seq in clinical samples.

Please cite this article as: Maria Sorokina et al, Diagnostic Utility of RNA-Seq for Evaluation of PD-L1 Expression in Clear Cell Renal Cell Carcinoma, Clinical Genitourinary Cancer, https://doi.org/10.1016/j.clgc.2021.07.010

Clinical Practice Points

- In the United States, RCC is in the top ten most commonly diagnosed cancers. ccRCC is the predominant histology of RCC, representing 75% of all cases.
- In this study, the sensitivity and clinical utility of RNA-Seq and IHC in PD-L1 detection was compared in a cohort of 127 ccRCC tumors; PD-L1 mRNA values and IHC analysis showed substantial agreement.
- Using knowledge-based gene expression signatures revealed two distinct ccRCC tumor microenvironments: an immune-enriched TME with high lymphocyte infiltration and an immune-desert TME predominantly composed of malignant cells.
- Patients with a higher expression of PD-L1, measured either by RNA-Seq or IHC, correlate with response to ICIs for ccRCC.
- Our data show that RNA-Seq detection of PD-L1 has potential utility in clinical samples of ccRCC. Therefore, future prospective studies will be critical to further validate PD-L1 measurements by RNA-Seq in clinical settings.

Disclosure

JJH has received consulting fees from Eisai and BostonGene; clinical trial funding from BMS, Merck USA, AstraZeneca, Exelixis, and SillaJen; and research funding from Merck USA, BostonGene, and TScan.

Credit Author Statement

Maria Sorokina: writing-original draft preparation and results discussion

Danil Stupichev: bioinformatics analysis and results discussion

Yang Lyu: data curation, bioinformatics analysis and results discussion

Akshaya Ramachandran: data curation and results discussion

Natalia Miheecheva: bioinformatics analysis and results discussion

Jessica H. Brown: manuscript preparation

Krystle Nomie: manuscript preparation

Ekaterina Postovalova: manuscript preparation, supervision and results discussion

Alexander Bagaev: manuscript preparation, supervision

Maria Tsiper: manuscript preparation and results discussion

James J. Hsieh: conceptualization, reviewing and editing

Acknowledgements

JJH and this work were supported by the National Institutes of Health [R01 CA223231].

References

1. Siegel RL, Miller KD, Jemal A. Cancer statistics, 2018. *CA Cancer J Clin*. 2018;68:7–30. doi:10.3322/caac.21442.
2. Voss MH, Reising A, Cheng Y, et al. Genomically annotated risk model for advanced renal-cell carcinoma: a retrospective cohort study. *Lancet Oncol*. 2018;19:1688–1698. doi:10.1016/S1470-2045(18)30648-X.
3. Hsieh JJ, Le V, Cao D, Cheng EH, Creighton CJ. Genomic classifications of renal cell carcinoma: a critical step towards the future application of personalized kidney cancer care with pan-omics precision. *J Pathol*. 2018;244:525–537. doi:10.1002/path.5022.
4. Huang JJ, Hsieh JJ. The therapeutic landscape of renal cell carcinoma: from the dark age to the golden age. *Semin Nephrol*. 2020;40:28–41. doi:10.1016/j.semnephrol.2019.12.004.
5. Hsieh JJ, Purdue MP, Signoretti S, et al. Renal cell carcinoma. *Nat Rev Dis Primer*. 2017;3:17009. doi:10.1038/nrdp.2017.9.
6. Feng X, Zhang L, Tu W, Cang S. Frequency, incidence and survival outcomes of clear cell renal cell carcinoma in the United States from 1973 to 2014: A SEER-based analysis. *Medicine (Baltimore)*. 2019;98:e16684. doi:10.1097/MD.0000000000016684.
7. Maeseneer DJD, Delafontaine B, Rottey S. Checkpoint inhibition: new treatment options in urologic cancer. *Acta Clin Belg*. 2017;72:24–28. doi:10.1080/17843286.2016.1260890.
8. Zhu J, Armstrong AJ, Friedlander TW, et al. Biomarkers of immunotherapy in urothelial and renal cell carcinoma: PD-L1, tumor mutational burden, and beyond. *J Immunother Cancer*. 2018;6:4. doi:10.1186/s40425-018-0314-1.
9. Kammerer-Jacquet S-F, Deleuze A, Saout J, et al. Targeting the PD-1/PD-L1 Pathway in Renal Cell Carcinoma. *Int J Mol Sci*. 2019;20. doi:10.3390/ijms20071692.
10. Torlakovic E, Lim HJ, Adam J, et al. Interchangeability" of PD-L1 immunohistochemistry assays: a meta-analysis of diagnostic accuracy. *Mod Pathol*. 2020;33:4–17. doi:10.1038/s41379-019-0327-4.
11. Motzer RJ, Robbins PB, Powles T, et al. Avelumab plus axitinib versus sunitinib in advanced renal cell carcinoma: biomarker analysis of the phase 3 JAVELIN Renal 101 trial. *Nat Med*. 2020;26:1733–1741. doi:10.1038/s41591-020-1044-8.
12. Mariathasan S, Turley SJ, Nickles D, et al. TGFβ attenuates tumour response to PD-L1 blockade by contributing to exclusion of T cells. *Nature*. 2018;554:544–548. doi:10.1038/nature25501.
13. Kim B, Lee C, Kim YA, Moon KC. PD-L1 expression in muscle-invasive urinary bladder urothelial carcinoma according to basal/squamous-like phenotype. *Front Oncol*. 2020;10. doi:10.3389/fonc.2020.527385.
14. Bray NL, Pimentel H, Melsted P, Pachter L. Near-optimal probabilistic RNA-seq quantification. *Nat Biotechnol*. 2016;34:525–527. doi:10.1038/nbt.3519.
15. Barrett T, Wilhite SE, Ledoux P, et al. NCBI GEO: archive for functional genomics data sets–update. *Nucleic Acids Res*. 2013;41:D991–D995 (Database issue). doi:10.1093/nar/gks1193.
16. Leinonen R, Sugawara H, Shumway M. International Nucleotide sequence database collaboration. the sequence read archive. *Nucleic Acids Res*. 2011;39:D19–D21 (Database issue). doi:10.1093/nar/gkq1019.
17. Uhlen M, Karlsson MJ, Zhong W, et al. A genome-wide transcriptomic analysis of protein-coding genes in human blood cells. *Science*. 2019;366. doi:10.1126/science.aax9198.
18. Blondel VD, Guillaume J-L, Lambiotte R, Lefebvre E. Fast unfolding of communities in large networks. *J Stat Mech Theory Exp*. 2008;2008:P10008. doi:10.1088/1742-5468/2008/10/P10008.
19. Grimm M-O, Leucht K, Grünwald V, Foller S. New first line treatment options of clear cell renal cell cancer patients with pd-1 or pd-l1 immune-checkpoint inhibitor-based combination therapies. *J Clin Med*. 2020;9. doi:10.3390/jcm9020565.
20. Hirsch FR, McElhinny A, Stanforth D, et al. PD-L1 Immunohistochemistry assays for lung cancer: results from phase 1 of the blueprint pd-l1 ihc assay comparison project. *J Thorac Oncol Off Publ Int Assoc Study Lung Cancer*. 2017;12:208–222. doi:10.1016/j.jtho.2016.11.2228.
21. Tsao MS, Kerr KM, Kockx M, et al. PD-L1 Immunohistochemistry comparability study in real-life clinical samples: results of blueprint phase 2 project. *J Thorac Oncol Off Publ Int Assoc Study Lung Cancer*. 2018;13:1302–1311. doi:10.1016/j.jtho.2018.05.013.
22. Eckstein M, Wirtz RM, Pfannstil C, et al. A multicenter round robin test of PD-L1 expression assessment in urothelial bladder cancer by immunohistochemistry and RT-qPCR with emphasis on prognosis prediction after radical cystectomy. *Oncotarget*. 2018;9:15001–15014. doi:10.18632/oncotarget.24531.
23. Abstract 4526: Predicting response: PD-L1 biomarker testing by IHC and RNA-seq | cancer research. Accessed March 8, 2021. https://cancerres.aacrjournals.org/content/78/13_Supplement/4526
24. Conroy JM, Pabla S, Nesline MK, et al. Next generation sequencing of PD-L1 for predicting response to immune checkpoint inhibitors. *J Immunother Cancer*. 2019;7:18. doi:10.1186/s40425-018-0489-5.
25. Tretiakova M, Fulton R, Kocherginsky M, et al. Concordance study of PD-L1 expression in primary and metastatic bladder carcinomas: comparison of four commonly used antibodies and RNA expression. *Mod Pathol Off J U S Can Acad Pathol Inc*. 2018;31:623–632. doi:10.1038/modpathol.2017.188.
26. Tsimafeyeu I, Imyanitov E, Zavalishina L, et al. Agreement between PDL1 immunohistochemistry assays and polymerase chain reaction in non-small cell lung cancer: CLOVER comparison study. *Sci Rep*. 2020;10:3928. doi:10.1038/s41598-020-60950-2.

Please cite this article as: Maria Sorokina et al, Diagnostic Utility of RNA-Seq for Evaluation of PD-L1 Expression in Clear Cell Renal Cell Carcinoma, Clinical Genitourinary Cancer, https://doi.org/10.1016/j.clgc.2021.07.010